Supporting Information

Polyoxotungstates Incorporating Organotriphosphonate Ligands and Lanthanide Ions: Syntheses, Characterization, Magnetism and Photoluminescence Properties

Ran Ban, Xiaopeng Sun, Jiawei Wang, Pengtao Ma, Chao Zhang, Jingyang Niu* and Jingping Wang*

Henan Key Laboratory of Polyoxometalate Chemistry,
Institute of Molecular and Crystal Engineering,
College of Chemistry and Chemical Engineering,
Henan University, Kaifeng, Henan 475004, People's Republic of China,
E-mail: jyniu@henu.edu.cn, jpwang@henu.edu.cn; Fax: (+86)371−23886876.

CONTENTS

Section1. IR spectra of **1Ce−4Eu**

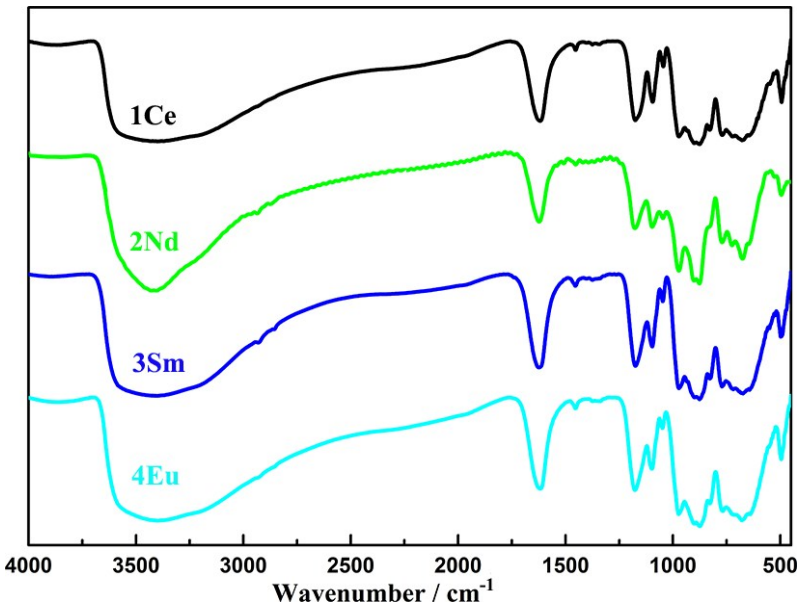

Fig. S1 IR spectra of **1Ce–4Eu**

Solid state IR spectra of **1Ce–4Eu** have been recorded between 4000 and 450cm^{-1} to investigate the structural characters of targeted samples (Fig. S1). The spectra are very similar to each other with only slight shifts in the position of the bands, indicating that **1Ce–4Eu** almost have the same basic framework, and that is in good agreement with the results of the single-crystal X-ray structural analysis. The characteristic peaks detected at 711, 775, 871 and 980 cm^{-1} for **1Ce**; 715, 763, 882 and 983 cm^{-1} for **2Nd**; 718, 763, 886 and 978 cm^{-1} for **3Sm**; 716, 768, 886 and 985 cm^{-1} for **4Eu**; are assigned to the vibrations of ν(W−O$_c$) , ν(W−O$_b$), ν(As−O$_a$) and ν(W−O$_t$), respectively. The absorption bands in the range 1184–1035 cm^{-1} of **1Ce–4Eu** are assigned to the vibration bands of P−O bonds, and the ones in the range 673–666 cm^{-1} are assigned to the vibrations of the P−C groups, which demonstrate the grafting of organic ligands onto the surface of POMs. The broad peaks around 3450 cm^{-1} for **1Ce−4Eu** are assigned to the stretching vibration ν(O–H), as well as signals appearing at 1618−1627 cm^{-1} are attributed to the bending vibration δ(O–H) of crystal and coordinated water molecules.

Section2. Powder X-ray diffraction patterns of simulated and experimental for **1Ce−4Eu**

The Powder X-ray diffraction (PXRD) patterns of **1Ce–4Eu** have been characterized by the good agreement with the simulated patterns derived from single-crystal X-ray diffraction (Fig. S2), implying the good phase purity for **1Ce−4Eu**. The disparities in intensity of some diffraction peaks may be attributed to the variation of preferred orientation of the powder sample during the course of collecting the experimental PXRD patterns.

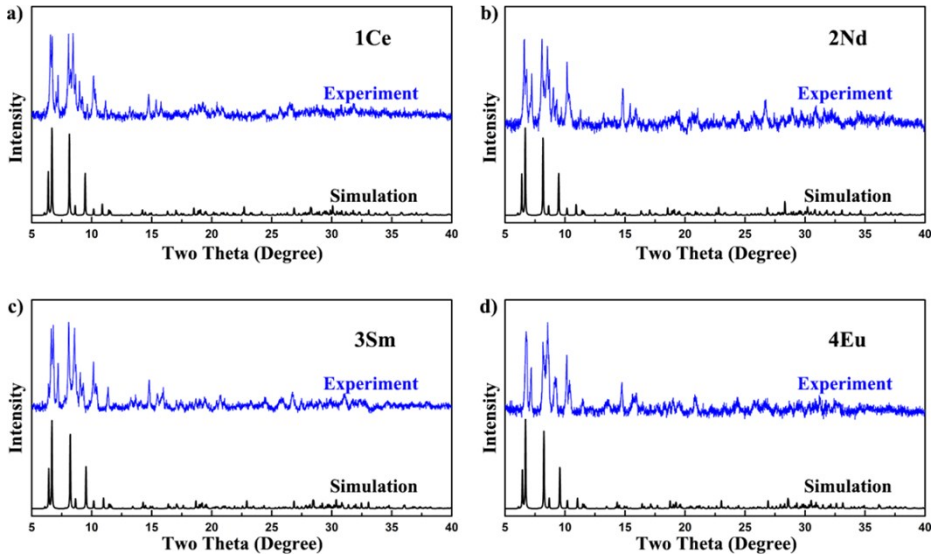

Fig. S2 Simulated (black) and experimental PXRD patterns (blue) of **1Ce−4Eu**

Section3. BVS values of selected oxygens atoms in **1Ce−4Eu**

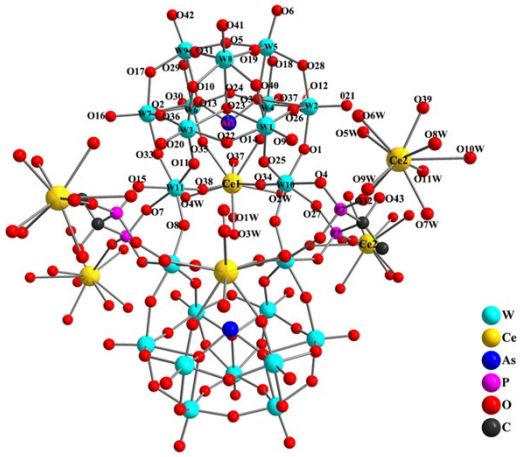

Fig. S3 Ball-and-stick representation of polyanion for **1Ce**

Table S1 BVS values of selected oxygens atoms in **1Ce−4Eu**

atom	BVS				protonation
	1Ce	**2Nd**	**3Sm**	**4Eu**	
O43	0.850	0.797	1.056	0.898	monoprotonated
O1W	0.348	0.318	0.349	0.321	diprotonated
O2W	0.341	0.363	0.358	0.361	diprotonated
O3W	0.305	0.305	0.288	0.322	diprotonated
O4W	0.354	0.334	0.349	0.359	diprotonated
O5W	0.339	0.328	0.346	0.323	diprotonated
O6W	0.282	0.292	0.328	0.310	diprotonated
O7W	0.400	0.333	0.417	0.365	diprotonated
O8W	0.359	0.336	0.365	0.396	diprotonated
O9W	0.379	0.320	0.264	0.355	diprotonated
O10W	0.136	0.618	0.587	0.546	diprotonated
O11W	0.297	0.194	0.205	0.229	diprotonated

Section4. EDX spectra of single crystal of **1Ce−4Eu** and EDX analyses

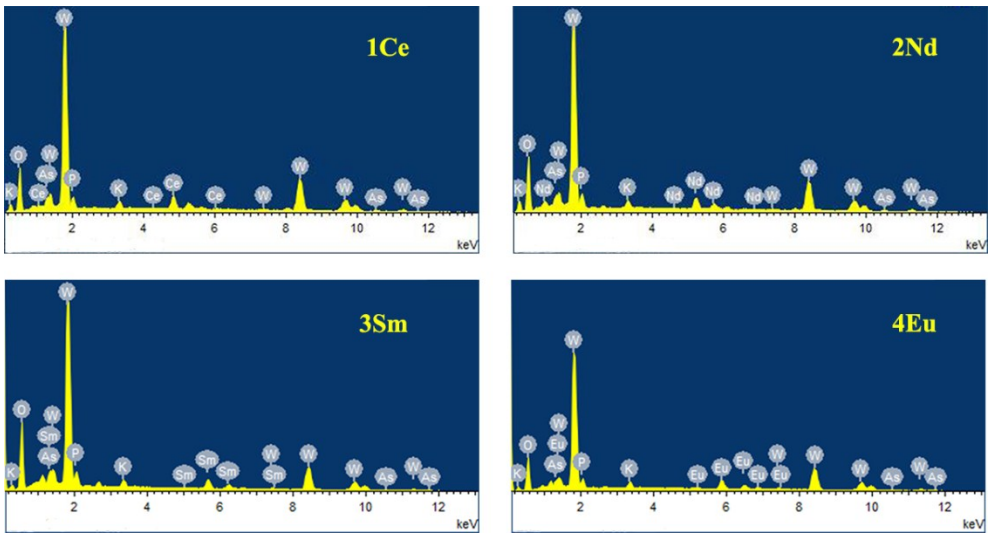

Fig. S4 EDX spectra of single crystal of **1Ce−4Eu**

EDX analyses

EDX was used to characterize the composition of **1Ce−4Eu** using single crystals. According to the EDX spectra, W : K and As : K were respectively detected with approximate ratio of 10.6 : 1, 0.97 : 1 and this result has been checked using multiple samples to reduce the error in the value. In consideration of the error of EDX measurements, we combine EDX, structural data, BVS analyses, magnetic property, TG analyses, elemental analyses and charge balance arguments to estimate the formula of the isostructural compounds **1Ce−4Eu**. Using these approach we can give the formula is $K_2[Ln(H_2O)_4(AsW_9O_{33})(W_2O_3)(O_3PCOHCH_3PO_3)Ln(H_2O)_7]_2{\cdot}15H_2O$ [Ln = Ce (**1Ce**), Nd (**2Nd**), Sm (**3Sm**) and Eu (**4Eu**)] (W：K = 11 : 1，As：K = 1 : 1).

Section5. The Ln−O bond lengths analyses with lanthanide contraction

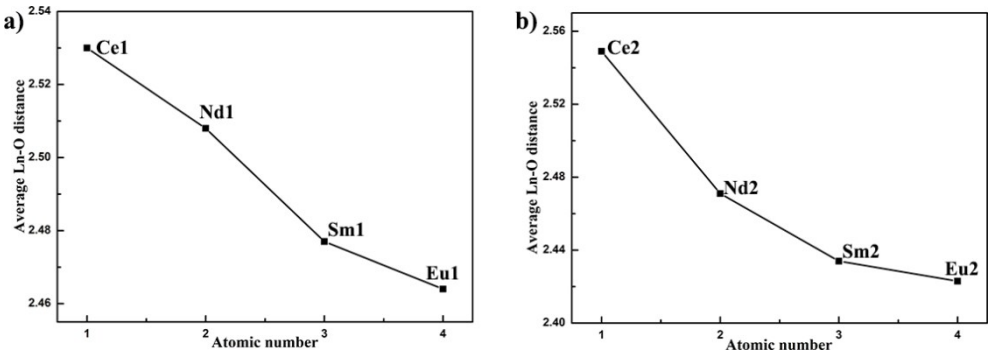

Fig. S5 The variation trend of Ln−O average bond lengths

Table S2 The average and bond lengths of Ln−O in **1Ce−4Eu**

Atom	Bond	Bond length (Å)	Average length (Å)	Atom	Bond	Bond length (Å)	Average length (Å)
Ce1	Ce1−O14	2.544(14)	2.530	**Ce2**	Ce2−O32	2.397(15)	2.549
	Ce1−O34	2.503(14)			Ce2−O39	2.353(16)	
	Ce1−O35	2.480(14)			Ce2−O5W	2.551(16)	

	Ce1−O37	2.479(14)			Ce2−O6W	2.62(2)	
	Ce1−O38	2.544(14)			Ce2−O7W	2.49(2)	
	Ce1−O1W	2.542(17)			Ce2−O8W	2.53(2)	
	Ce1−O2W	2.549(18)			Ce2−O9W	2.51(2)	
	Ce1−O3W	2.59(2)			Ce2−O10W	2.89(4)	
	Ce1−O4W	2.535(17)			Ce2−O11W	2.60(3)	
	Nd1−O14	2.502(9)			Nd2−O32	2.372(10)	
	Nd1−O34	2.500(9)			Nd2−O39	2.335(11)	
	Nd1−O35	2.486(9)			Nd2−O5W	2.506(12)	
	Nd1−O37	2.493(9)			Nd2−O6W	2.543(17)	
Nd1	Nd1−O38	2.528(9)	2.508	**Nd2**	Nd2−O7W	2.494(18)	2.471
	Nd1−O1W	2.529(11)			Nd2−O8W	2.492(17)	
	Nd1−O2W	2.480(13)			Nd2−O9W	2.510(17)	
	Nd1−O3W	2.544(13)			Nd2−O10W	2.28(3)	
	Nd1−O4W	2.511(12)			Nd2−O11W	2.71(2)	
	Sm1−O14	2.47(2)			Sm2−O32	2.29(2)	
	Sm1−O34	2.47(2)			Sm2−O39	2.31(2)	
	Sm1−O35	2.47(2)			Sm2−O5W	2.47(3)	
	Sm1−O37	2.45(2)			Sm2−O6W	2.49(3)	
Sm1	Sm1−O38	2.49(2)	2.477	**Sm2**	Sm2−O7W	2.40(4)	2.434
	Sm1−O1W	2.47(2)			Sm2−O8W	2.45(3)	
	Sm1−O2W	2.46(3)			Sm2−O9W	2.57(3)	
	Sm1−O3W	2.54(3)			Sm2−O10W	2.27(7)	
	Sm1−O4W	2.47(3)			Sm2−O11W	2.66(6)	
	Eu1−O14	2.465(11)			Eu2−O32	2.326(13)	
	Eu1−O34	2.468(11)			Eu2−O39	2.308(12)	
	Eu1−O35	2.476(12)			Eu2−O5W	2.473(14)	
	Eu1−O37	2.426(12)			Eu2−O6W	2.50(2)	
Eu1	Eu1−O38	2.473(11)	2.464	**Eu2**	Eu2−O7W	2.44(2)	2.423
	Eu1−O1W	2.489(14)			Eu2−O8W	2.41(2)	
	Eu1−O2W	2.446(16)			Eu2−O9W	2.45(2)	
	Eu1−O3W	2.488(15)			Eu2−O10W	2.29(3)	
	Eu1−O4W	2.448(14)			Eu2−O11W	2.61(4)	

Section6. Thermal gravimetric analyses of **1Ce**−**4Eu**

Thermal gravimetric analyses (TGA) of the four compounds have been analyzed upon heating to 800 °C under N_2 atmosphere (Fig. S6). All the TG curves show two slow steps of weight loss, the first weight loss of 9.18% for **1Ce** (calcd 9.45%), 8.97% for **2Nd** (calcd 9.43%), 9.62% for **3Sm** (calcd 9.39%) and 9.53% for **4Eu** (calcd 9.38%) in the temperature of 25−380 °C, respectively, which correspond to the release of fifteen crystal water molecules and twenty-two coordinated water molecules. From 380 to 800 °C, the second weight loss of 3.98% (calcd 4.05%), 4.48% (calcd 4.04%), 4.64% (calcd 4.03%) and 4.17% (calcd 4.03%) for **1Ce**−**4Eu**, respectively,

can be ascribed to the loss of two {–$COHCH_3$} groups and the sublimation of As_2O_3 molecules.

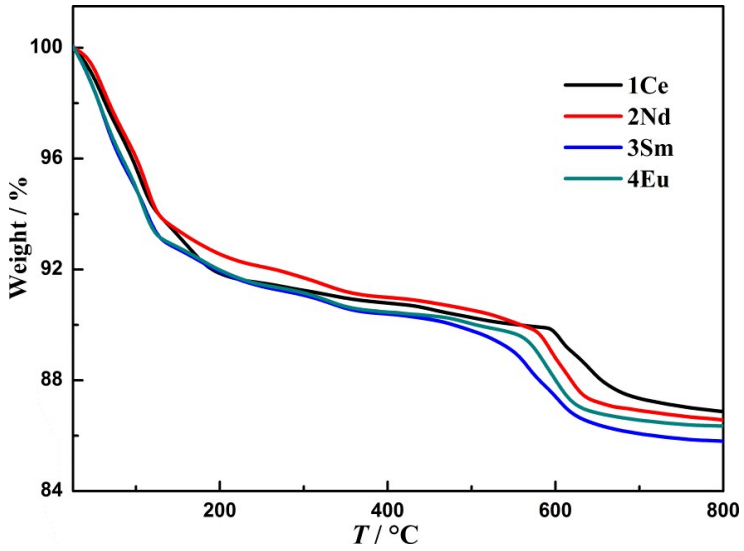

Fig. S6 TG curves of **1Ce**−**4Eu**

Section7. The $1/\chi_M$ versus T plots and the best-fit by the Curie-Weiss law for **1Ce** and **2Nd**

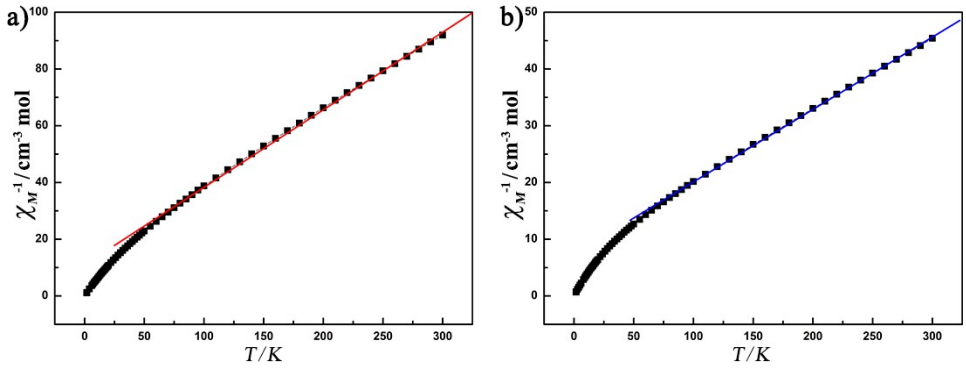

Fig. S7 The temperature dependence of $1/\chi_M$ for **1Ce** (a) and **2Nd** (b), and the red solid for **1Ce** and the blue solid for **2Nd** lines represent the best-fit by the Curie-Weiss law.

Section8. Some other additional figures

Fig. S8 The crescent inorganic-organic hybrid module {$(W_2O_3)(O_3PCOHCH_3PO_3)Ce(H_2O)_7$}

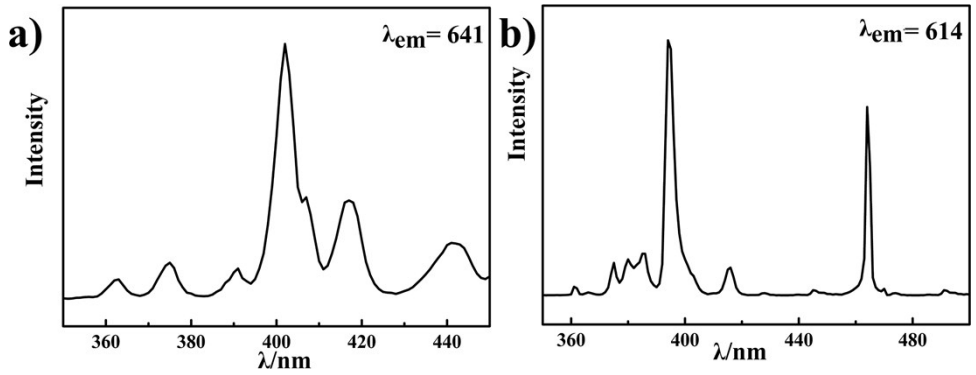

Fig. S9 Excitation spectra of **3Sm** (a) and **4Eu** (b) in the solid state at room temperature.

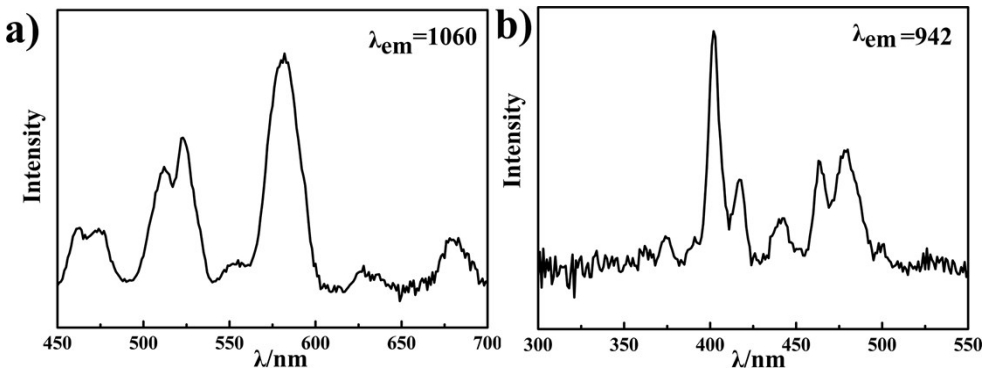

Fig. S10 The NIR excitation spectra of **2Nd** (a) and **3Sm** (b) in solid state at room temperature

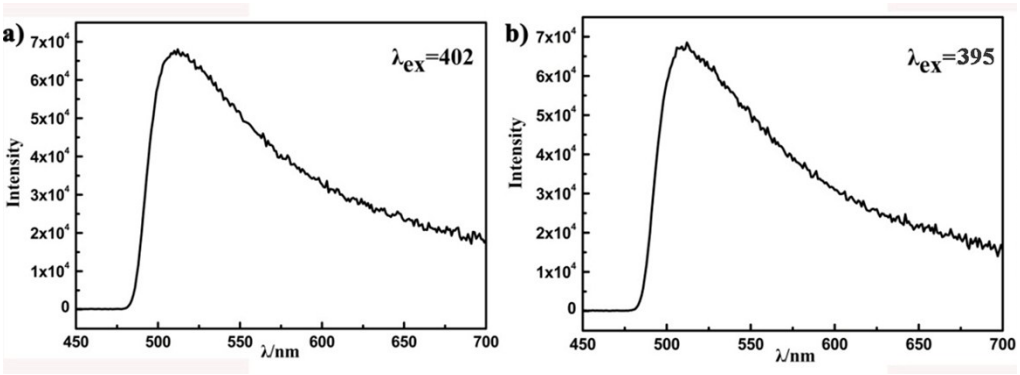

Fig. S11 (a) The solid-state emission spectrum of $\{As_2W_{19}\}$ under a light of 402 nm, (b)The solid-state emission spectrum of $\{As_2W_{19}\}$ under a light of 395 nm.

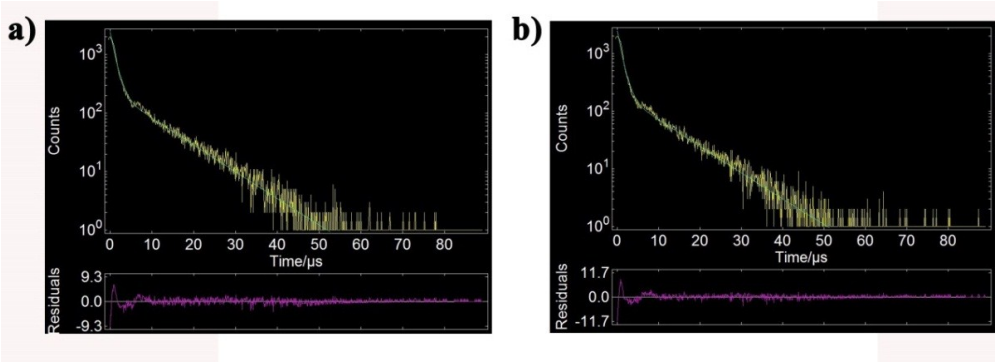

Fig. S12 (a) The decay curve of $\{As_2W_{19}\}$ under the excitation at 402 nm, (b) The decay curve of $\{As_2W_{19}\}$ under the excitation at 395 nm.

Section9. CIE color chromaticity coordinates of **3Sm** and **4Eu**

The CIE 1931 diagram is a international standard approach for studying all the possible colors by combining the three primary colors, in which the chromaticity coordinates *x* and *y* are always used to confirm the exact emission color for the tested samples. The CIE chromaticity coordinates (*x*, *y*) for **3Sm** and **4Eu** are identified on the basis of the corresponding photoluminescence spectra and are indexed to (0.60368, 0.39432) and (0.64901, 0.34968), respectively (Fig. S11), which can be easily observed the reddish orange for **3Sm** and red for **4Eu**.

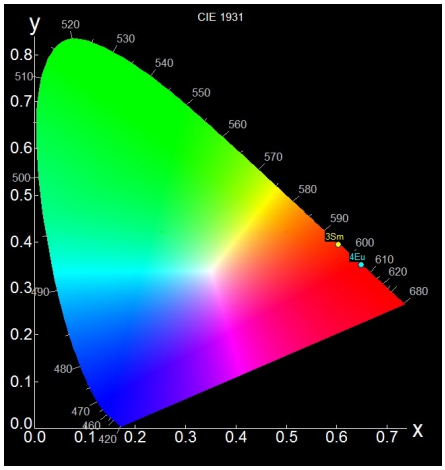

Fig. S13 The CIE chromaticity diagrams of **3Sm** and **4Eu**.